

Research article

Turbostratic carbon supported palladium as an efficient catalyst for reductive purification of water from trichloroethylene

Emil Kowalewski¹, **Małgorzata Zienkiewicz-Machnik**¹, **Dmytro Lisovytskiy**¹, **Kostiantyn Nikiforov**¹, **Krzysztof Matus**², **Anna Śrębowata**^{1,*}, and **Jacinto Sá**^{1,3,*}

¹ Institute of Physical Chemistry, Polish Academy of Sciences, Kasprzaka 44/52, 01-224 Warsaw, Poland

² Institute of Engineering Materials and Biomaterials, Silesian University of Technology, Konarskiego 18A, 44-100 Gliwice, Poland

³ Department of Chemistry, Ångström Laboratory, Uppsala University, Uppsala 75120, Sweden

* **Correspondence:** Email: jacinto.sa@kemi.uu.se; Tel: +46-18-471-68-06; asrebowata@ichf.edu.pl; Tel: +48-22-2433320.

Abstract: This work investigates the catalytic properties of turbostratic carbon supported Pd catalyst in hydrodechlorination of trichloroethylene (TCE HDC) in aqueous phase. 1.57 wt% Pd/C was thoroughly characterized by BET, TPHD, CO chemisorption, PXRD, STEM, XPS and used as the catalyst in removal of trichloroethylene from drinking water in batch and continuous-flow reactors. The studies showed that catalytic performance of Pd/C depended on the hydrophobicity and textural properties of carbon support, which influenced noble metal dispersion and increased catalyst tolerance against deactivation by chlorination. Palladium in the form of uniformly dispersed small (~3.5 nm) nanoparticles was found to be very active and stable in purification of water from TCE both in batch and continuous-flow operation.

Keywords: palladium catalyst; turbostratic carbon; batch reactor vs. continuous-flow reactions; water purification; hydrodechlorination

1. Introduction

Palladium, thanks to its hydrogenolytic properties, is still extensively used in catalytic hydrogenation processes [1,2], such as hydrodechlorination (HDC), a very important technological

and environmental process [3,4]. Water purification by HDC is preferable method to counteract the increasing water pollution by mutagenic and cancerogenic chloroorganic compounds, e.g., trichloroethylene (TCE) [4–8]. Although HDC is often considered as a structural sensitive reaction, clear correlations between Pd particles size and their activity in aqueous phase HDC remains largely unknown and controversial. For example, several studies found that an increase of the active phase particles size leads to an increase of HDC rate, both in gas and in liquid phase [9–12]. However, there are other studies that several authors reported a beneficial role of the small Pd particles on overall activity of metallic catalysts [13].

Besides of the active phase, support plays a significant role in the HDC process [3,4,5,12]. Carbon materials, due to their high adsorption capacity for organic compounds and high stability under the aggressive conditions of the reaction, are often the supports of choice for HDC water purification [12]. In accordance to literature [14,15], application of the materials with ordered structure as the supports of metallic phase affected their stability and activity. The high surface area of ordered mesoporous materials used as supports can be exploited to create highly dispersed active species on their surface. All of these properties make them excellent materials in an aqueous-phase hydrodechlorination of chloroorganic compounds. Moreover, deprived of a vast majority of functional (e.g., oxygen-carrying) groups, a strongly hydrophobic nature of highly pretreated carbon would help in more effective adsorption of TCE from wastewaters. Subsequent hydrodechlorination on Pd sites located in the porous structure of carbon should efficiently transform this harmful molecule into more benign products as it was reported earlier [16]. A final aspect relates to the *modus operandi*. Majority of the scientific reports concerns processes in batch mode [4,11], with very little attention paid to flow conditions [5], despite the potential benefits from process scalability and adaptability.

The aim of this study was to develop an active and stable palladium catalyst with small NPs stabilized in turbostratic carbon support, which could be used in the reductive purification of water from chloroorganic contaminant, both in batch and continuous-flow reactor. Our work was focused on trichloroethylene as a widely used solvent, degreaser and substrate for the synthesis, classified as a human carcinogen by the U.S. Environmental Protection Agency (U.S. EPA) [17]. TCE metabolism to mutagenic and toxic moieties [18] and its interaction with very popular drugs such as naproxen and salicylic acid, which could increase TCE metabolites levels, causes different adverse responses every living organism to this chloroorganic compound [19]. Due to the fact, that the main source of TCE is water, our investigations seem to be justifiable.

2. Materials and Method

2.1. Catalyst Preparation and Characterization

Commercial amorphous carbon Norit CNR 115 with specific surface area $1860 \text{ m}^2/\text{g}$ and pore volume $1.05 \text{ cm}^3/\text{g}$ (supplied by Norit B.V. Company) was used as a starting material in the support synthesis. Norit CNR115 was modified by a two-step procedure to obtained carbon support with hallmarks of turbostraticity. The first step was the heating of raw carbon pellets in argon at 2173 K for 2 h, and the second step was the gasification of the obtained material in the stream of steam-argon at 1129 K, which resulted in mass loss up to 26.54 wt%. The obtained carbon material was washed with distilled water, dried in air at 393 K and was used as the support for the synthesis of the palladium

catalyst. 1.57 wt% Pd/C catalyst was synthesized by incipient wetness impregnation of turbostratic carbon material by the aqueous solution of PdCl₂.

The surface areas and porosities of carbon materials were measured with ASAP 2020 instrument from Micromeritics, employing the BET (Brunauer-Emmett-Teller), t-Plot, BJH (Barret-Joyner-Halenda) and HK (Horwath-Kawazoe) methods using nitrogen as adsorbate. Before measurement of the adsorption isotherm at 77 K, both carbon and Pd/C were kept at 573 K for 3 h in vacuum to clean their surfaces.

The particles sizes were determined based on CO and H₂ chemisorption at 308 K in Micromeritics ASAP 2020. Before measurement the sample was reduced for 2 h at 573 K in H₂ stream and then evacuated for 2 h at 593 K.

The fresh and spent Pd samples for transmission electron microscopy (TEM) measurement were prepared by dispersing the material in ethanol, placing it in an ultrasonic bath and then putting droplets of dispersed material onto copper grids coated with a film of amorphous carbon and dried in air at room temperature. TEM observations were performed on a probe Cs-corrected S/TEM Titan 80-300 FEI microscope with EDAX EDS detector. The images were recorded in STEM-mode, using the high-angle annular dark field (HAADF) detector and an electron beam with a convergence semi-angle of 24 mrad at 300 keV. HAADF is a ring-shaped detector used to collect electrons scattered at a large angle. In this situation, contrast is proportional to the square of the electric charge of the nucleus ($I(\chi) \sim Z^2$). HAADF detector can distinguish the crystallites containing elements with different Z value thanks to the difference in contrast.

Powder X-ray diffraction (PXRD) measurements were performed employing Bragg-Brentano configuration. This type of arrangement was provided using PANalytical Empyrean diffraction platform, powered at 40 kV × 40 mA and equipped with a vertical goniometer, with theta–theta geometry using Nifiltered Cu K α radiation. The data were collected in the range of $2\theta = 10\text{--}90^\circ$, with step size of 0.008° and counting time 60 s/step.

Temperature-programmed reduction (TPR) of catalyst precursor was followed by mass spectrometry (MA200, Dycor-Ametek, Pittsburgh, USA). TPR run was performed by flowing a 10% H₂/He mixture (25 ml/min) at a 10 °C/min ramp. During monitoring liberated species in the course of TPR, attention was focused on changes in $m/z = 2$ (hydrogen consumption) and $m/z = 36$, originating from released/decomposed/hydrogenated chloride precursor.

Temperature-programmed hydride decomposition (TPHD) for palladium catalyst was performed in glass flow system equipped with Gow-Mac thermal conductivity detector. Decomposition of palladium hydride, prior formed in 10% H₂/Ar stream, was observed during heating in range 293–433 K.

X-ray photoelectron spectroscopy (XPS) measurements were performed using a VG Scientific photoelectron spectrometer ESCALAB-210 using Al K α radiation (1486.6 eV) from an X-ray source operating at 14.5 kV and 25 mA. The survey spectra were recorded for all the samples in the energy range from 0 to 1350 eV with 0.4 eV step. High resolution spectra were recorded with 0.1 eV step, 100 ms dwell time and 25 eV pass energy. Ninety degrees take-off angle was used in all measurements. The curve fitting was performed using the AVANTAGE software provided by Thermo Electron, which describes each component of the complex envelope as a Gaussian-Lorentzian sum function; a constant 0.3 (± 0.05) G/L ratio was used. The background was fitted using nonlinear Shirley model. Scofield sensitivity factors and measured transmission function were used for quantification.

2.2. Catalytic Tests

The reductive purification of water in batch mode was performed under atmospheric pressure at room temperature (303 K) in a glass reactor equipped with: a magnetic stirring bar, pH-meter and a temperature controller. Every time 350 ml of MiliPore water was saturated with hydrogen for 30 minutes before adding TCE (20 μ l). Prior to catalyst addition (0.15 g), the reaction mixture was stirred (1000 rpm) for 30 minutes to provide homogeneity. The reaction samples were taken at 0, 2, 5, 10, 15, 20, 60, 90, 120 and 150 min of the reaction. Additional experiments were conducted without access to hydrogen.

Catalytic hydrodechlorination of TCE in flow mode was performed using ThalesNano H-Cube Pro continuous-flow micro-reactor. TCE solution in MiliPore water (83 ppm of TCE) was flown through 0.3 g of the catalyst with a flow rate of 1 ml/min, which results in supplying 0.64 μ mol of TCE per minute. The catalyst was placed in a 70 mm long stainless steel cartridge (CatCart®70) with an ID of 4 mm. The hydrogen was generated in situ via water electrolysis. The reaction was conducted at 303 K under 10 bar of hydrogen for 25 h. The LHSV (liquid hourly space velocity) for the conducted reactions was estimated and it was found to be 68. Additional experiments were conducted for 0.01 g of the sample (Pd/C and C) placed in a 30 mm long stainless steel cartridge and for the same concentration of TCE solution (83 ppm of TCE) for 300 minutes.

Catalytic tests, both in batch and flow mode, were repeated three times, to confirm catalyst's activity and stability. The concentration of substrate and the products were determined in headspace by gas-chromatographic set-up (Headspace SHS-40 and Bruker 456GC equipped with ECD and FID detectors with SolGel-WAX column: 30 m \times 0.25 mm, 0.25 μ m)

3. Results and Discussion

The textural parameters of the carbon material have shown that the first step of the modification of parent CNR115 led to a considerable carbon graphitization and a drastic decrease of the specific surface area (from 1860 to 16 m²/g) and pore volume (from 1.05 to 0.005 ml/g). After the gasification in the stream of steam-argon, the specific surface area and pore volume were equal to 1530 m²/g and 0.97 ml/g, respectively. Additionally, the formation of the parallel graphene layers was observed on TEM image (Figure 1).

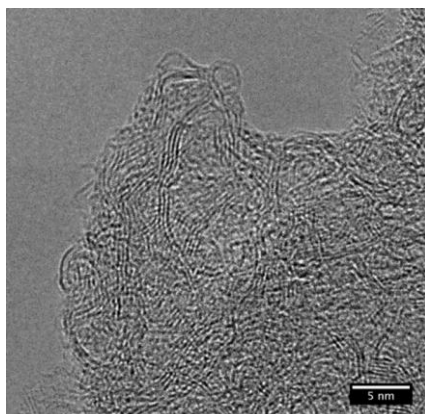


Figure 1. TEM image of the turbostratic carbon structure.

Figure 2 shows the nitrogen adsorption-desorption isotherm for the final carbon material. As we can see, the shape of N₂ adsorption isotherm of “gasified” carbon differs from a typical “langmuirian” shape. The hysteresis loop, indicates the presence of mesopores in carbon support.

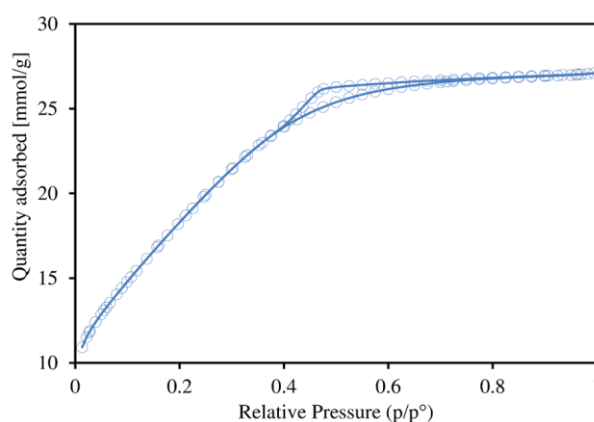


Figure 2. The nitrogen adsorption-desorption isotherm for turbostratic carbon material.

Figure 3 illustrates the BET determined pore width and pore volume (pore size distribution) shows both the presence of micropores and mesopores in the tested material. The impregnation of Pd on the turbostratic carbon support led to the reduction in the surface area, pore volume and averaged pore diameter (Table 1). This is likely attributed to the filling/blockage of the pores of the carbon support by Pd particles.

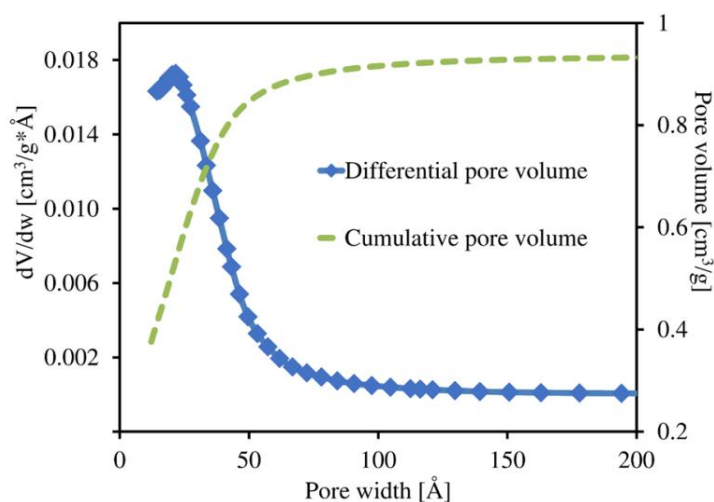


Figure 3. BET for plotting of pore size distribution for turbostratic carbon material.

Table 1. BET Surface area, pore volume and average pore diameter of carbon support and Pd/C catalyst.

Sample	Surface area [m ² /g]	Pore volume [cm ³ /g]	Averaged Pore Diameter [Å]
Carbon support	1530	0.97	24.5
1.57 wt% Pd/C	1520	0.92	24.3

H₂-TPR result obtained for 1.57 wt% Pd/C (Figure 4) means that, the conditions used in this study (10% H₂/Ar, 673 K, 2 h) should be sufficient for the complete reduction of carbon-supported palladium catalyst. TPR profile generated for 1.57 wt% Pd/C (Figure 4) clearly shows the presence of one dominant negative peak related to Pd-hydride phase, albeit with maximum at rather high temperature (ca. 420 K) compared with the earlier studies [20]. There are two main explanations for this phenomenon: i) the presence of the big palladium particles or ii) the ordering of the support [21]. Since Pd dispersion is very good (32% equating to an average particles size of 3.5 nm Pd NPs) based on the CO chemisorption, the most logical explanation for the shift of the Pd-hydride phase decomposition to higher temperature is associated with the use of turbostratic carbon as the support.

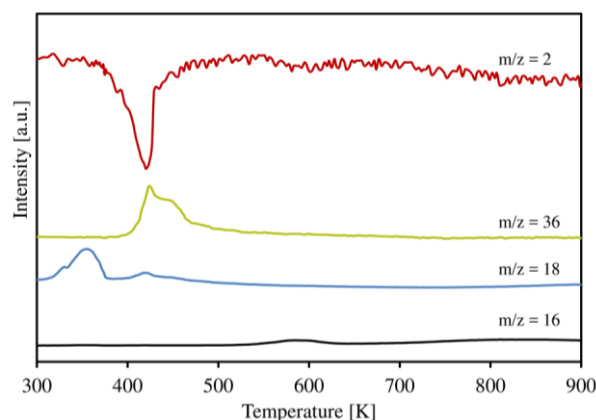


Figure 4. TPR patterns of Pd/C.

TPHD (temperature programmed hydride decomposition) method was investigated to assessment of the homogeneity of Pd particles size. This method uses the phenomenon of a facile β -PdH formation at a relatively low hydrogen pressure. The obtained results were interpreted based on the earlier studies of Bonarowska et al. [20]. A single TPHD peak shown in Figure 5 implies the β -PdH decomposition from similar in size palladium particles. In addition, a presence of the peak maximum at 344 K could indicate the existence of small Pd particles [20], in agreement with CO chemisorption and STEM results.

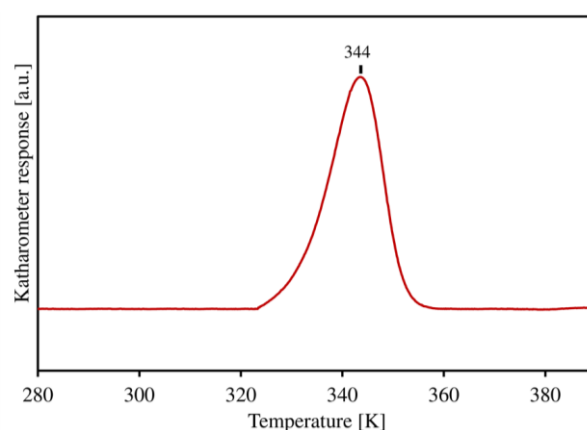


Figure 5. Temperature-programmed hydride decomposition (TPHD) profile of Pd/C.

The aqueous phase catalytic hydrodechlorination of TCE was carried out without any additional organic solvent, at relatively low reaction temperature (303 K). The blank tests, both in batch and flow reactor, confirmed that the chloroorganic compound removal did not occur in the absence of the activated carbon or palladium catalyst. Figure 6 shows the results of the catalytic removal of trichloroethylene from water in batch conditions as the changes of C/C_0 in time. As we can see, both pure carbon and palladium catalysts showed good properties in purification of water. After 150 minutes of the process approximately 60% and 90% of TCE had been removed from water, for C and Pd/C respectively. However, it should be mentioned here, that pure carbon material with a very high specific surface area, pore volume (Table 1) and ordered structure has shown good efficiency only of trichloroethylene sorption and products formation was not detected. Curve plateau observed after 100 min for the carbon material is the consequence of the sorption equilibrium reached. The introduction of 1.57 wt% Pd led to hydrodechlorination of TCE. According to our earlier studies [22], both the presence of 100% of hydrocarbons: 98.7% of C_2H_6 and 1.2% of C_2H_4 as reaction products and the decreasing of pH value during the time indicated that hydrodechlorination process had occurred. Carefully analysis of the catalytic results and negligible changes in the pH values after 100 min of the reaction could suggest about not sufficient amounts of hydrogen in the reaction mixture. Moreover, our studies were extended to additional experiments without hydrogen, for both Pd/C and C. Figure 6 clearly shows that independently on the used material, processing without hydrogen is limited to the TCE sorption. The curve plateau for Pd/C is reached in the same time and for the similar value of C/C_0 as for carbon support.

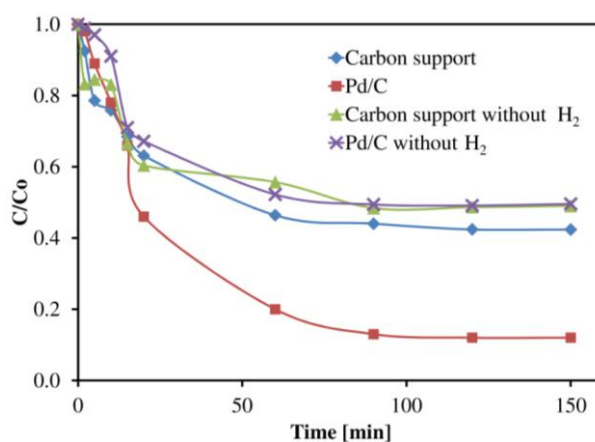


Figure 6. Evolution of TCE sorption and kinetics of TCE hydrodechlorination in the presence of Pd/C in batch reactor.

The aqueous phase hydrodechlorination of trichloroethylene on Pd/C could be assumed as pseudo-first-order due to the predominant amounts of hydrogen compared to trichloroethylene. However, due to the high carbon capacity, the kinetic data calculated for palladium catalyst take into account both sorption processes on carbon support and catalytic hydrodechlorination on Pd active centers [23,24]. The reaction rate constant k was calculated to be 0.027 s^{-1} and the initial reaction rate $1.98 \text{ mmol/min g}_{Pd}$. Additionally TOF value (0.01 s^{-1}) calculated according to the earlier studies of Molina et al. [25] proved to be similar to those reported in the literature for aqueous phase HDC with rather small Pd NPs [4,25]. The differences in the aqueous phase hydrodechlorination procedures

used by research groups make it difficult compare directly our results with the available data. However, our results obtained for aqueous phase hydrodechlorination of trichloroethylene at low reaction temperature and without any additional solvent can be considered satisfactory.

Keeping in mind that there is an increased interest in performing hydrogenation reactions and in particular HDC in flow mode [1,5], we made the decision to test the batch catalyst in a liquid continuous flow reactor using TCE concentrations exceeding 8000 times the acceptable level of the substance in drinking water. Figure 7 shows that both carbon material and palladium catalyst had effectively purified water during >1500 min of the process. The sorption properties of carbon had decreased in time, and after the first 300 minutes stabilized on a level $C/C_0 \sim 1$. On the other hand, 100% of the efficiency showed Pd/C without any symptoms of deactivation.

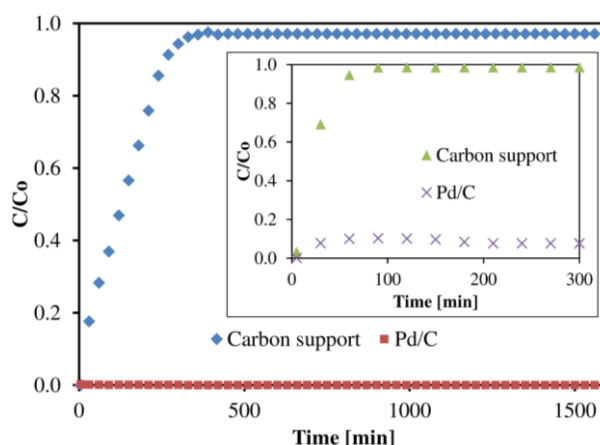


Figure 7. Evolution data for TCE sorption on C support and HDC of TCE catalytic activity over Pd/C in continuous flow liquid-phase. In insert similar experiments but carried out with 0.01 g of sample instead of 0.3 g.

The very high overall conversion of trichloroethylene obtained for palladium catalyst confers an important role of the textural properties of carbon materials on the catalytic behavior of Pd/C in hydrotreatment process. Moreover, additional experiment conducted with very low amount of Pd/C (0.01 g) but the same concentration of TCE shows that only in this case conversion below 100% can be achieved (Figure 7 insert). Our results are in line with the earlier studies [14,15], where the activity of mesoporous carbons supported metallic phase had been associated with the presence of metal particles confined in the ordered mesopores with a narrow pore distribution. Additionally, its turbostraticity and hydrophobicity makes Pd/C considerably resistant to ionic poisons, such as chloride ions, similarly like it was reported earlier for other hydrophobic materials [5,11]. Consequently, the application of the hydrophobic ordered carbon material could protect active phase against various ionic poisons existing in groundwater, and *ipso facto* could increase the performance of palladium catalyst.

Comparison of batch and flow reactors is not straightforward, due to the different factors that determined both *modus operandi*. Although, batch mode allows removing higher amounts of TCE per unit of time, the continuous flow catalytic proficiencies have the potential to decrease the transfer time from research to application. Moreover, the catalyst was found to be very stable based on the fact that 100% TCE removal performance was kept over >25 h.

Figure 8 shows the X-ray diffraction patterns for fresh and spent palladium catalyst. The lack of clear Pd related diffraction peaks in any of the samples suggests that its NPs are small in size, in accordance to the STEM image (Figure 9), and that they remain small after reaction. Additionally, the presence of turbostratic two dimensional ordering: first (0 0 2) peak with maximum at $\sim 24.2^\circ$ and next a single (1 0 0) peak, at $\sim 43.5^\circ$ for Pd/C at different stages of its biography means that, the aqueous phase hydrodechlorination of trichloroethylene did not affect the turbostratic character of carbon support.

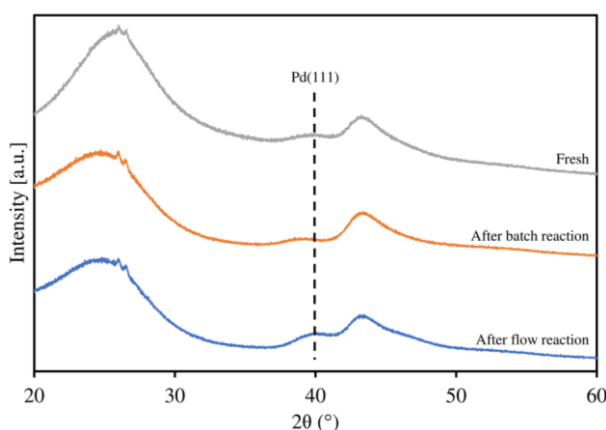


Figure 8. PXRD pattern for 1.57 wt% Pd/C after reduction and after TCE hydrodechlorination in batch and continuous flow reactor.

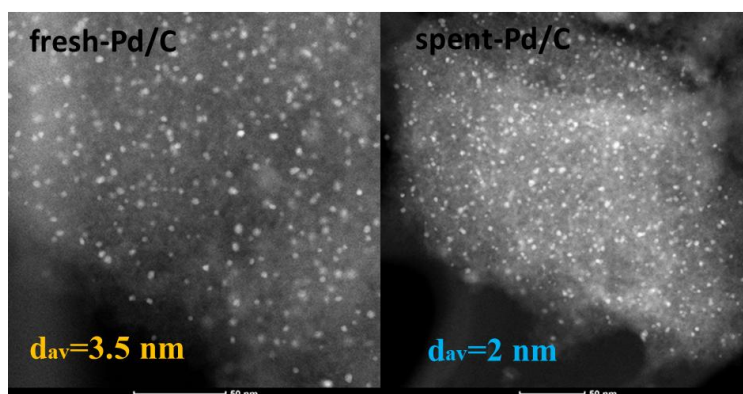


Figure 9. STEM image of fresh- and spent-Pd/C catalyst.

Comparative study of the TEM results obtained for fresh- and spent-Pd/C showed the presence of uniformly dispersed palladium nanoparticles with an average size of ~ 3.5 nm for fresh and ~ 2 nm for spent catalyst (Figure 9). Additionally, for the sample after catalytic run, the difference between Pd particles size was more visible. Except the nanoparticles similar in shape and size to those observed for fresh catalysts, lots of particles with much smaller dimensions were detected (Figure 9). STEM results indicate the decreasing of Pd NPs under reaction conditions. The decrease of NPs size and their redispersion during HDC is in agreement with previous studies with carbon supported noble metals catalysts [26,27]. This phenomenon is most often explained by influence of HCl, which

contribute to the formation of mobile metallic chlorides. Ordoñez et al. [26] observed redispersion for carbon supported Pd and Pt catalysts in the HDC of tetrachloroethylene, while Álvarez-Montero et al. [27] only for Pt/C in chloromethanes hydrodechlorination.

Analysis of XPS spectra (Figure 10) obtained for the Pd/C after reduction step and after long term reaction. The dominant signal of Pd 3d_{5/2} on the freshly reduced catalyst located at 335.9 eV relates to Pd in metallic form. The signal is slightly shifted to higher binding energy indicating small metallic NPs [28]. The Pd 3d_{5/2} binding energy of spent sample was found to be 337.0 eV, which is a clear indication for the presence of Pd²⁺ ions, possibly in the form of PdCl₂, which is corroborated by the presence of Cl 2p signal. This suggests that reaction mechanism involves palladium surface chlorination, which is subsequently cleaned by hydrogen spillover leading to the formation of gaseous HCl. Hydrogen spillover in aqueous phase was also suggested as the crucial step of nitrates hydrogenation reaction [29] Additionally, the spent catalyst showed a 10% decrease in palladium carbon ratio, which suggests carbon deposition as aforementioned.

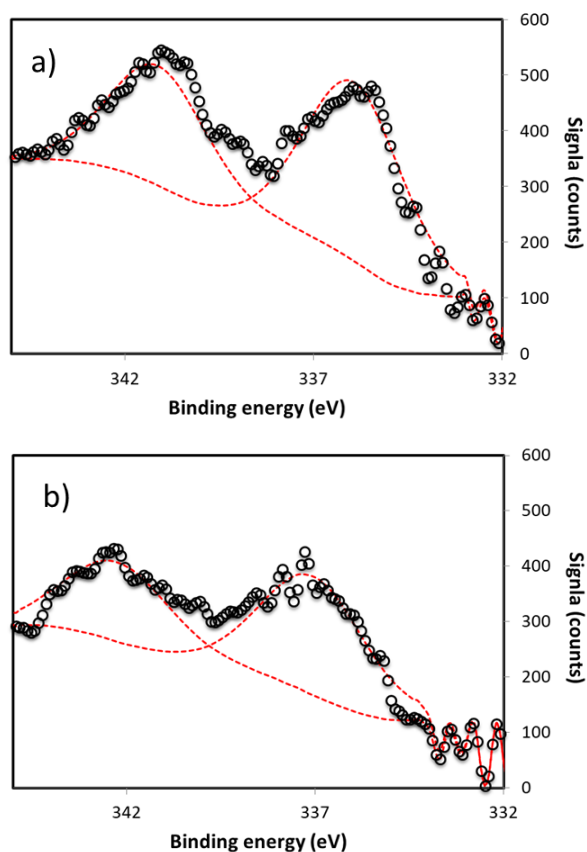


Figure 10. XPS of palladium catalyst after reduction step (a) and after catalytic reaction (b). Narrow scan of Pd 3d region.

4. Conclusion

Catalytic performance of the turbostratic carbon supported nano-Pd catalyst has been evaluated in aqueous phase hydrodechlorination of trichloroethylene. Our results clearly show that Pd/C is able to catalytically purify water from chloroorganic compounds both in batch and continuous flow

reactor. The hydrophobicity and textural parameters of carbon support play an important role in activity and stability of Pd/C catalyst.

Acknowledgments

This work was partially sponsored by the Institute of Physical Chemistry, Polish Academy of Sciences in Warsaw and partially sponsored by National Science Centre in Poland within the project UMO-2014/15/B/ST5/02094. We would like to thank Wioletta Raróg-Pilecka from Technical University in Warsaw for turbostratic carbon synthesis.

Conflict of Interest

The authors declare that they have no conflict of interests in this work.

References

1. Goszewska I, Giziński D, Zienkiewicz-Machnik M, et al. (2017) A novel nano-palladium catalyst for continuous-flow chemoselective hydrogenation reactions. *Catal Commun* 94: 65–68.
2. McCue AJ, Guerrero-Ruiz A, Rodríguez-Ramos I, et al. (2016) Palladium sulphide—A highly selective catalyst for the gas phase hydrogenation of alkynes to alkenes. *J Catal* 340: 10–16.
3. Munoz M, Kolb V, Lamolda A, et al. (2017) Polymer-based spherical activated carbon as catalytic support for hydrodechlorination reactions. *Appl Catal B-Environ* 218: 498–505.
4. Kamińska I, Lisovytskiy D, Casale S, et al. (2017) Influence of preparation procedure on catalytic activity of PdBEA zeolites in aqueous phase hydrodechlorination of 1,1,2-trichloroethene. *Micropor Mesopor Mat* 237: 65–73.
5. Sohn H, Celik G, Gunduz S, et al. (2017) Hydrodechlorination of trichloroethylene over Pd supported on swellable organically-modified silica (SOMS). *Appl Catal B-Environ* 203: 641–653.
6. Sahu RS, Li D, Doong R (2018) Unveiling the hydrodechlorination of trichloroethylene by reduced graphene oxide supported bimetallic Fe/Ni nanoparticles. *Chem Eng J* 334: 30–40.
7. Sahu RS, Bindumadhavan K, Doong R (2017) Boron-doped reduced graphene oxide-based bimetallic Ni/Fe nanohybrids for the rapid dechlorination of trichloroethylene. *Environ Sci-Nano* 4: 565–576.
8. Yu X, Wu T, Yang XJ, et al. (2016) Degradation of trichloroethylene by hydrodechlorination using formic acid as hydrogen source over supported Pd catalysts. *J Hazard Mater* 305: 178–189.
9. Juszczak W, Malinowski A, Karpiński Z (1998) Hydrodechlorination of CCl₂F₂ (CFC-12) over γ -alumina supported palladium catalysts. *Appl Catal A-Gen* 166: 311–319.
10. Aramendía MA, Boráu V, García IM, et al. (1999) Influence of the Reaction Conditions and Catalytic Properties on the Liquid-Phase Hydrodechlorination of Chlorobenzene over Palladium-Supported Catalysts: Activity and Deactivation. *J Catal* 187: 392–399.
11. Baeza JA, Calvo L, Gilarranz MA, et al. (2012) Catalytic behavior of size-controlled palladium nanoparticles in the hydrodechlorination of 4-chlorophenol in aqueous phase. *J Catal* 293: 85–93.

12. D áz E, Faba L, Ord óñez S (2011) Effect of carbonaceous supports on the Pd-catalyzed aqueous-phase trichloroethylene hydrodechlorination. *Appl Catal B-Environ* 104: 415–417.
13. Ren Y, Fan G, Wang C (2014) Aqueous hydrodechlorination of 4-chlorophenol over an Rh/reduced graphene oxide synthesized by a facile one-pot solvothermal process under mild conditions. *J Hazard Mater* 274: 32–40.
14. Śrębowata A, Kamińska II, Giziński D, et al. (2015) Remarkable effect of soft-templating synthesis procedure on catalytic properties of mesoporous carbon supported Ni in hydrodechlorination of trichloroethylene in liquid phase. *Catal Today* 251: 60–65.
15. Letellier F, Blanchard J, Fajerweg K, et al. (2006) Search for confinement effects in mesoporous supports: hydrogenation of o-xylene on Pt/MCM-41. *Catal Lett* 110: 115–124.
16. Bonarowska M, Rar óg-Pilecka W, Karpiński Z (2011) The use of active carbon pretreated at 2173 K as a support for palladium catalysts for hydrodechlorination reactions. *Catal Today* 169: 223–231.
17. Guha N, Loomis D, Grosse Y, et al. (2012) International Agency for Research on Cancer Monograph Working Group, Carcinogenicity of trichloroethylene, tetrachloroethylene, some other chlorinated solvents, and their metabolites. *Lancet Oncol* 13: 1192–1193.
18. Lash LH, Chiu WA, Guyton KZ, et al. (2014) Trichloroethylene biotransformation and its role in mutagenicity, carcinogenicity and target organ toxicity. *Mutat Res-Rev Mutat* 762: 22–36.
19. Rouhou MC, Haddad S (2014) Modulation of trichloroethylene in vitro metabolism by different drugs in human. *Toxicol In Vitro* 28: 732–741.
20. Bonarowska M, Pielaszek J, Semikolenov VA, et al. (2002) Pd–Au/Sibunit Carbon Catalysts: Characterization and Catalytic Activity in Hydrodechlorination of Dichlorodifluoromethane (CFC-12). *J Catal* 209: 528–538.
21. Amorim C, Keane MA (2008) Palladium supported on structured and nonstructured carbon: A consideration of Pd particle size and the nature of reactive hydrogen. *J Colloid Interf Sci* 322: 196–208.
22. Śrębowata A, Tarach K, Girman V, et al. (2016) Catalytic removal of trichloroethylene from water over palladium loaded microporous and hierarchical zeolites. *Appl Catal B-Environ* 181: 550–560.
23. Munoz M, Kaspereit M, Etzold BJM (2016) Deducing kinetic constants for the hydrodechlorination of 4-chlorophenol using high adsorption capacity catalysts. *Chem Eng J* 285: 228–235.
24. Munoz M, Zhang GR, Etzold BJM (2017) Exploring the role of the catalytic support sorption capacity on the hydrodechlorination kinetics by the use of carbide-derived carbons. *Appl Catal B-Environ* 203: 591–598.
25. Molina CB, Pizarro AH, Casas JA, et al. (2014) Aqueous-phase hydrodechlorination of chlorophenols with pillared clays-supported Pt, Pd and Rh catalysts. *Appl Catal B-Environ* 148–149: 330–338.
26. Ord óñez S, Díez F, Sastre H (2001) Characterisation of the deactivation of platinum and palladium supported on activated carbon used as hydrodechlorination catalysts. *Appl Catal B-Environ* 31: 113–122.
27. Álvarez-Montero MA, Gómez-Sainero LM, Mayoral A, et al. (2011) Hydrodechlorination of chloromethanes with a highly stable Pt on activated carbon catalyst. *J Catal* 279: 389–396.

-
28. Bertolini JC, Delichere P, Khanra BC, et al. (1990) Electronic properties of supported Pd aggregates in relation with their reactivity for 1,3-butadiene hydrogenation. *Catal Lett* 6: 215–223.
29. Ilinicha OM, Gribov EN, Simonov PA (2003) Water denitrification over catalytic membranes: hydrogen spillover and catalytic activity of macroporous membranes loaded with Pd and Cu. *Catal Today* 82: 49–56.



AIMS Press

© 2017 Jacinto S á Anna Śrębowata, et al., licensee AIMS Press. This is an open access article distributed under the terms of the Creative Commons Attribution License (<http://creativecommons.org/licenses/by/4.0>)